Surface diffusion of Pb atoms on the Si(553)-Au surface in narrow quasi-one-dimensional channels

P. Nita

Instituto Madrileno de Estudios Avanzados en Nanociencia (IMDEA Nanociencia), Campus Universitario de Cantoblanco, Calle Faraday 9, 28049 Madrid, Spain

K. Palotás

Department of Theoretical Physics, Budapest University of Technology and Economics, Budafoki út 8., H-1111 Budapest, Hungary and Condensed Matter Research Group of the Hungarian Academy of Sciences, Budafoki út 8., H-1111 Budapest, Hungary

M. Jałochowski and M. Krawiec[*]

Institute of Physics, M. Curie-Skłodowska University, Pl. M. Curie-Skłodowskiej 1, 20-031 Lublin, Poland
(Received 28 January 2014; published 28 April 2014)

The one-dimensional diffusion of individual Pb atoms on the Si(553)-Au surface has been investigated by a combination of scanning tunneling microscopy (STM), spectroscopy (STS), and first-principles density functional theory. The obtained results unambiguously prove that the diffusion channels are limited to a narrow region between Au chains and step edges of the surface. Much wider channels observed in STM and STS data have electronic origin and result from an interaction of Pb with surface atoms. The length of the channels is determined by a distance between defects at step edges of the Si(553)-Au surface. The defects can act as potential barriers or potential wells for Pb atoms, depending on their origin.

I. INTRODUCTION

Atomic diffusion has been studied for a long time as one of the fundamental processes governing the surface physics [1–6]. For example, the diffusion of atoms is responsible for epitaxial growth of atomic layers, formation of islands, chains, and other nanostructures or chemical reactions. Many different mechanisms of diffusion have been identified up to now, like thermally activated hopping, exchange of atoms, and quantum-mechanical tunneling, to name a few. Usually, at low surface coverage of adsorbate atoms, the movement of atoms is uncorrelated and proceeds via hopping of individual atoms. At higher coverage, the situation is more complicated as the hopping may become correlated due to interactions between the adatoms.

Usually, the diffusion of atoms on low-index surfaces is two dimensional and rather isotropic, like in the case of various adsorbates on the Si(111) surface [7–22]. However, the movement of atoms can become strongly anisotropic or even quasi-one-dimensional in the presence of a specific surface reconstruction or on stepped (vicinal) templates [23–28].

Recently, using scanning tunneling microscopy (STM), we have discovered the one-dimensional diffusion of Pb atoms on the Si(553)-Au surface at temperatures above 110 K [26]. Due to a regular morphology of the Si(553)-Au surface, featuring equally spaced steps and a low number of defects [29–32], it was possible to observe an unusual long-range one-dimensional mobility of individual Pb atoms. The STM topography images show that Pb atoms move along the step edges on long distances, several dozens nanometers or even longer, limited by defects. No jumps across the steps have been observed at room temperature. According to density functional theory (DFT) calculations [26,27], the diffusion channels are composed of shallow energy barrier series, ranging from 0.18

to 0.42 eV. In the perpendicular direction the movement of Pb atoms is limited by as high as 1 eV energy barriers, which explains the absence of interchannel jumps in the experiment. Furthermore, the diffusion trajectories of Pb atoms determined by DFT calculations are located near step edges of the surface, i.e., between the step-edge Si atoms and double Au chains (see Fig. 4 of Ref. [26]). However, the constant current STM topography images do not show such behavior. Instead, the STM topography signal coming from diffusing Pb atoms is recorded almost across the whole terrace (see Fig. 2 of Ref. [26]). Thus it is not clear if the diffusion channels are really located near the step edges of the surface. Moreover, the STM topography data suggest that the channels are much wider than predicted by DFT calculations.

In the present work we unambiguously prove that the diffusion of individual Pb atoms on the Si(553)-Au surface is confined to narrow channels located between the step edges and the double Au chains and explain the origin of much wider diffusion channels observed in STM topography. The STM current maps together with measured and calculated current-voltage characteristics fully support the idea of narrow terraces near step edges. The widening of the channels observed in STM topography has mainly electronic origin due to the interaction of Pb atoms with the neighboring surface atoms. The second purpose is to study the influence of defects on the diffusion of atoms. The defects modify substantially diffusion processes and act as potential barriers or potential wells for Pb atoms, depending on their type. They also determine the length of the diffusion channels. A very good agreement between the theoretical results and the experimental data confirms the above scenario.

The rest of the paper is organized as follows. Experimental details and theoretical approach are described in Sec. II. Results of STM and STS measurements together with theoretical calculations are presented and discussed in Sec. III. We end up with conclusions in Sec. IV.

---

*mariusz.krawiec@umcs.pl

II. EXPERIMENT AND DETAILS OF CALCULATIONS

The experiments were performed in an ultrahigh vacuum (UHV) chamber at pressures $<10^{-10}$ mbar, equipped with an Omicron VT scanning tunneling microscope, reflection high energy electron diffraction (RHEED) apparatus, a quartz crystal microbalance, and several evaporation cells. The STM tips were chemically etched tungsten tips shortly annealed in an UHV condition by thermal side contact with Ta filament heated to about $900\,^\circ$C. The sample was cut from n-type P-doped Si(553) wafer with a room temperature resistivity of $0.14\ \Omega$ cm. The Si(553) sample was carefully degassed several hours by heating with automatically controlled direct current while keeping the pressure below $<2 \times 10^{-10}$ mbar. Final cleaning of the bare Si(553) was performed by repeated cycles of flashing to $\sim$1550 K under the RHEED control until a clean surface without SiC contamination was achieved. Next, 0.48 ± 0.02 ML of Au [in units of one half of the Si(111) surface atom density equal to 7.84×10^{14} atoms/cm^2] Au was deposited onto the substrate held at room temperature (RT). The desired well-ordered surface in the form of one-dimensional structures running along the periodically arranged atomic steps was obtained after heating the sample at 950 K for 20 s and gradual cooling to the room temperature over 3 min. A small amount of Pb of $\sim$0.01 ML, was then evaporated on Si(553)-Au at RT.

The calculations were performed within local density approximation (LDA) to density functional theory [33], as implemented in SIESTA code [34–38]. Troullier-Martins norm-conserving pseudopotentials were used [39]. In the case of Au and Pb atoms the semicore $5d$ states and scalar relativistic corrections were included. A double-ζ polarized (DZP) basis set was used for all the atomic species [35,36]. Six nonequivalent k points for Brillouin zone sampling and a real-space grid equivalent to a plane-wave cutoff 100 Ry have been used.

The Si(553)-Au slab has been modeled by four silicon double layers and a vacuum region of 19 Å. All the atomic positions were fully relaxed until the maximum force in any direction was less than 0.01 eV/Å, except the bottom layer. The Si atoms in the bottom layer were fixed at their bulk ideal positions and saturated with hydrogen. The lattice constant of Si was fixed at the calculated value, 5.39 Å. Most of the results are presented for single Pb atom per 1×2 unit cell, containing a single terrace of the Si(553)-Au surface and $2 \times a_{[1\bar{1}0]}$ long in direction parallel to the steps. The $a_{[1\bar{1}0]} = 3.81$ Å is the Si-Si distance in the direction $[1\bar{1}0]$. The diffusion of Pb atoms was studied in 1×12 unit cell. Details of the atomic structure can be found in Ref. [30].

The STM simulations were performed by using the three-dimensional Wentzel-Kramers-Brillouin electron tunneling model implemented in the 3D-WKB-STM code [40–42]. The model was extended for the treatment of f-electron orbitals, i.e., including the real spherical harmonics of $f_{3x^2y-y^3}, f_{xyz}, f_{yz^2}, f_{5z^3-3z}, f_{xz^2}, f_{x^2z-y^2z}, f_{x^3-3xy^2}$, for the Pb atom. We considered a blunt tungsten tip model following Ref. [43]. In simulations the electron work functions, 4.93 eV [bare Si(553)-Au surface], 4.30 eV (Pb-covered surface), and 4.80 eV (W blunt tip), obtained by DFT calculations were adapted.
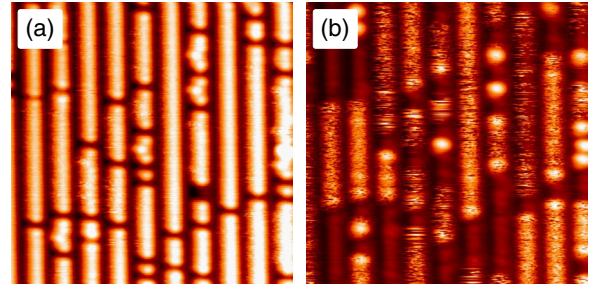

FIG. 1. (Color online) STM topography images of the same area, 15×15 nm^2, of the Si(553)-Au surface covered by 0.01 ML Pb recorded at (a) $U = -2.1$ V and at (b) $U = +2.1$ V.

III. RESULTS AND DISCUSSION

Figure 1 shows the (a) filled and (b) empty states STM topography images of the same area of the Si(553)-Au surface, recorded at temperature $T = 220$ K. As it was discussed in Ref. [26], the filled states STM topography [Fig. 1(a)] reproduces well the morphology of the bare Si(553)-Au surface, i.e., before the deposition of Pb. The observed chain structures come from the step-edge Si atoms [30]. On the other hand, at positive sample bias [Fig. 1(b)], two sets of atomic chains appear: the dark chains of the native Si(553)-Au surface, visible also at negative polarization, and bright Pb chains (compare the structural model in Fig. 2). The bright chains in Fig. 1(b) look fuzzy and strongly modulated, which is an indication that Pb atoms move fast along the step edges, as discussed in Ref. [26]. We shall return to this problem later on.

The fact that Pb chains are visible only at positive sample bias has its origin in electronic properties of Pb atoms. Namely, the electron density of states (DOS) of Pb atoms is strongly asymmetrical with respect to the Fermi energy (E_F), with very high DOS in the empty state region. On the other hand, the step-edge Si atoms show an opposite behavior, featuring higher DOS below the E_F. This is illustrated in Fig. 3, where the DOS projected on different atoms (PDOS) is plotted. Due to the charge transfer between Pb adatoms and the surface, the Pb PDOS features the empty $6p$ states and the step-edge Si PDOS—the occupied $3p$ states. Thus at positive sample bias the STM records mainly the Pb atoms, while at
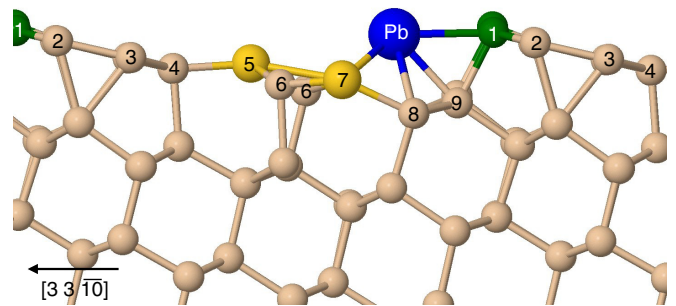

FIG. 2. (Color online) The structural model of adsorbed Pb atoms on Si(553)-Au surface. The surface atoms are numbered from 1 to 9. Lead atom (Pb) is shown blue, gold atoms (5 and 7)—orange, step-edge Si atoms (1)—green, and rest of Si atoms—light-green color. The atoms Si1 to Si4 form the honeycomb chain (HC).
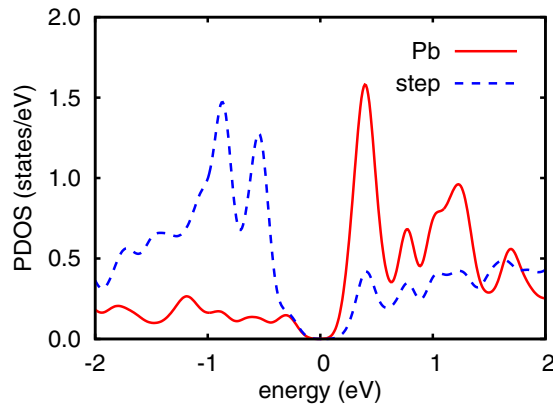
FIG. 3. (Color online) The calculated projected density of states (PDOS) of Pb (red solid curve) and the step-edge Si atoms (blue dashed curve). Fermi energy is set to zero.

negative polarization—the step-edge Si atoms. Such behavior is confirmed by simulated STM images, presented in Fig. 4. Clearly, at negative sample bias the highest STM intensities of the bare and Pb-covered Si(553)-Au surface coincide to each other [compare Figs. 4(a) and 4(c)]. At positive bias Pb atoms are better visible than step-edge Si atom chains [Fig. 4(d)].

To further verify the above scenario, we have calculated a single point current-voltage characteristics. Figure 5 shows a comparison of the $I(V)$ curve for Pb adatom and the bare surface at the position of Pb adatom. As expected from the PDOS behavior, a high current flows into the empty states of Pb adatoms. Note that in the case of Pb adatom the current at positive sample bias is an order of magnitude larger than for bare surface, while at negative bias there is no strong difference.

Such behavior of the $I(V)$ characteristics gives another opportunity to study the diffusion of Pb atoms. Namely, when acquiring STS data at a fixed position over the surface, the moving Pb atom should change the magnitude of the tunneling current, and thus influence the shape of the $I(V)$ curve. As a result, we expect a switching of $I(V)$ characteristic between
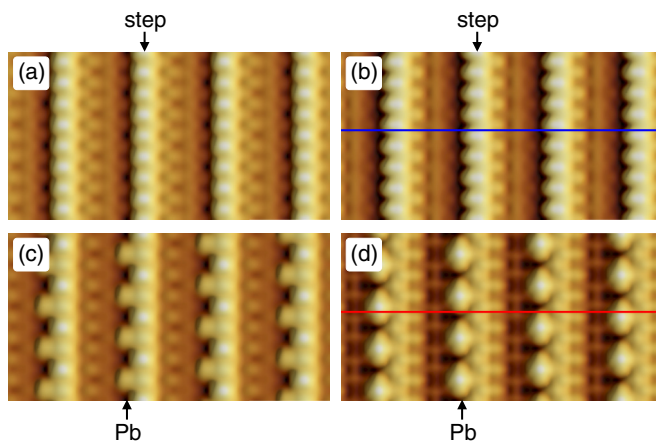

FIG. 4. (Color online) 5.9×3.0 nm^2 STM simulations of the bare [(a) and (b)] and Pb-covered Si(553)-Au surface [(c) and (d)]. (a) and (c) show the filled state ($U = -1.22$ V), and (b) and (d) the empty state constant current topography ($U = +1.22$ V). The highest intensity is shown light. Blue and red lines in right panels mark the lines along which the profiles of Fig. 8 are plotted.
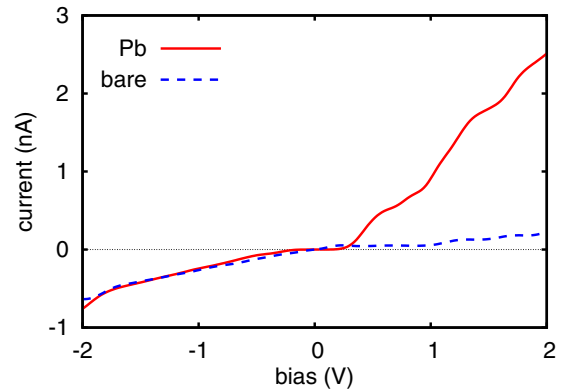

FIG. 5. (Color online) The calculated single point current-voltage characteristics of the Pb adatom (red solid curve) and the bare surface (blue dashed curve) at the position of Pb adatom.

a high current due to Pb atom present below the STM tip, and a low current in absence of the Pb atom. Indeed, exactly this behavior is observed in measured STS data. Figure 6 shows the STS characteristics together with a current map with marked positions where the STS data were collected. In the Pb-free region of the surface, the $I(V)$ characteristics are smooth and show rather a low current flowing (five bottom black curves in left panel). On the other hand, in the region with Pb atom diffusing, each of the five STS curves switches between the high-current and the low-current states, clearly indicating the presence and absence of Pb atom below the STM tip. Naturally, the switching is responsible for the fuzzy and strongly modulated topography with many streaks observed in the empty state topography in Fig. 1 and in current map (Fig. 6). Of course, the switching was observable only with
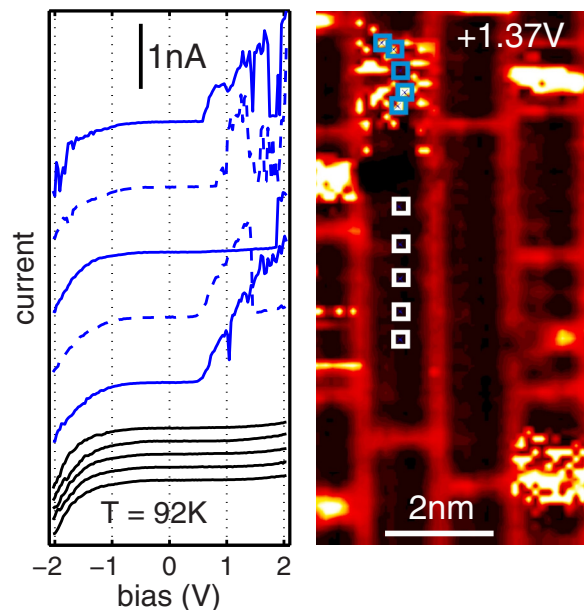

FIG. 6. (Color online) The STS current-voltage characteristics (left panel) and corresponding current map with the indicated positions where the $I(V)$ curves were recorded. The bottom black curves in left panel were acquired at positions marked by white squares in the right panel, while the top blue curves in blue squares. Note a switching of the $I(V)$ curves due to the diffusion of Pb atoms.

a proper choice of the recording time of $I(V)$ characteristics with respect to the speed of the moving Pb atoms. If the time was too short we could measure either the high-current state or the low-current state. On the other hand, if the time was too long, the $I(V)$ characteristics are expected to be averaged and noisy, thus contain very little information.

Now a question arises about the position of the diffusion channel. The DFT calculations show that the whole diffusion trajectory is located near the step edges (see Fig. 4(b) of Ref. [26]). Moreover, the Pb atoms make bonds with the step-edge Si1 and Au7 atoms (see Fig. 2) along the diffusion path, as discussed in Ref. [27]. This results in a slightly shifted Pb chains in the direction $[33\overline{1}0]$ with respect to the step-edge Si chains, as observed in Fig. 1(b). The simulated constant-current topography images, shown in Fig. 4, confirm this scenario. The measured current maps also support such a view. Figure 7 shows the current map (a) recorded at the bias voltage $U = 1.89$ V with corresponding line profiles across the steps (b). Indeed, whenever the Pb atom is present and moves along the steps, the position of the maximal value of the current is shifted in the direction $[33\overline{1}0]$, i.e., toward the left in the figure. It is the best illustrated when comparing the first and third maxima. At the first maximum, the diffusion of Pb atoms is present in the red solid rectangle, thus the first red solid line peak of the line profile is shifted toward the left with respect to the blue dashed one. The situation is opposite in the case of the third peak. Now the diffusion region is covered by the blue dashed rectangle, thus the line profile blue dashed peak is also shifted to the left.

Correspondingly calculated line profiles are shown in Fig. 8. Clearly the same behavior is observed, i.e., the shifted position of Pb chains (red curve) with respect to the step edges of the

FIG. 8. (Color online) The calculated constant-height line profiles along the lines indicated in Fig. 4. Note that Fig. 4 represents the constant-current topography.

Si(553)-Au surface (blue curve). Such behavior is in a perfect agreement with the conclusion that Pb atoms move in channels near the step edges. All the above shows that the diffusion of Pb atoms performs near steps of the Si(553)-Au surface.

According to the DFT calculations (see also Refs. [26,27]), the diffusion channel is quite narrow. The Pb trajectory is always located between the step-edge and the double Au chain (see Fig. 2). On the other hand, the STM topography (Fig. 1), or even more the current map of Fig. 7 suggests that the diffusion takes place on a large part of the surface terrace. Of course, one can argue that this effect is mainly associated with the presence of an STM tip and a nature of tunneling in this system, i.e., tunneling with different **k** vectors. Certainly this may result in observed widening of an investigated surface object. However, we shall point to another possibility associated with bonding of Pb atoms to the step-edge and Au-chain structures and hybridization of their states. The adsorption of Pb atom changes the electronic structure of neighboring region, which in turn can influence the STM signal. Thus the apparent widening of the Pb diffusion channel can be observable if the electronic states of Pb adatom hybridize with the states of neighboring surface atoms. Indeed, this happens in the present case. Figure 9 shows modifications of calculated PDOS of different atoms upon adsorption of a single Pb atom (per unit cell) in its lowest energy configuration (see Fig. 2). Recalling that the adsorbed Pb atom features a high PDOS around 0.5–1 eV above the Fermi energy and looking for changes of PDOS of other atoms in this energy region, we arrive at the conclusion that PDOS of almost all the surface atoms is modified. The strongest modifications are observed in the case of the HC structure (Si1-Si4) and Au7 atoms. The electronic empty states of all these atoms give rise to higher STM current at positive sample bias, thus widen the apparent width of Pb diffusion channels.

Finally, we would like to shed some light on the length of the diffusion channels. As it was already mentioned and also discussed in Refs. [26,27], the movement of Pb atoms along the step edges is limited by the presence of defects. To check if defects can suppress or even block the diffusion of atoms we have performed DFT calculations in much longer unit cell, i.e., 1×12. We have considered two types of defects: a vacancy and a protrusion. The vacancy was obtained by removing a single
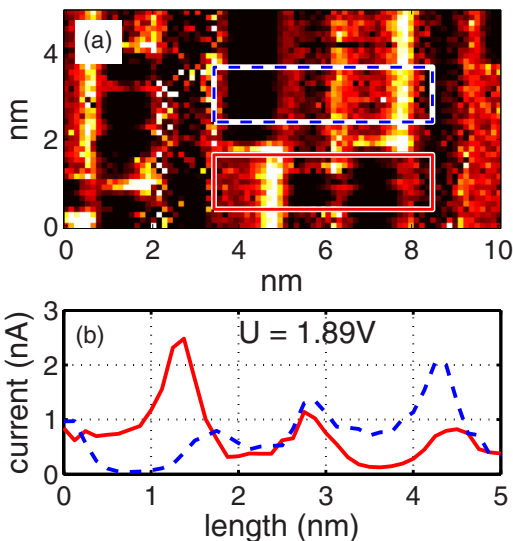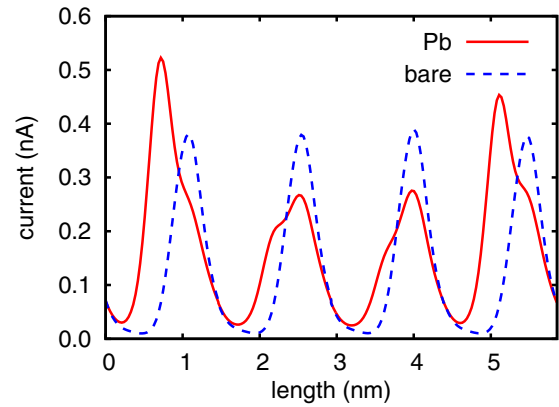

FIG. 7. (Color online) The current map (a) recorded at the bias voltage $U = 1.89$ V and corresponding line profiles across the steps of the Si(553)-Au surface with diffusing Pb atoms (b). The profiles were acquired and averaged along the step edges over the rectangles indicated in (a). The red solid (blue dashed) profile in (b) corresponds to the red solid (blue dashed) frame in (a), respectively. Note the different positions of maximal values of the current due to the diffusion of Pb atoms.
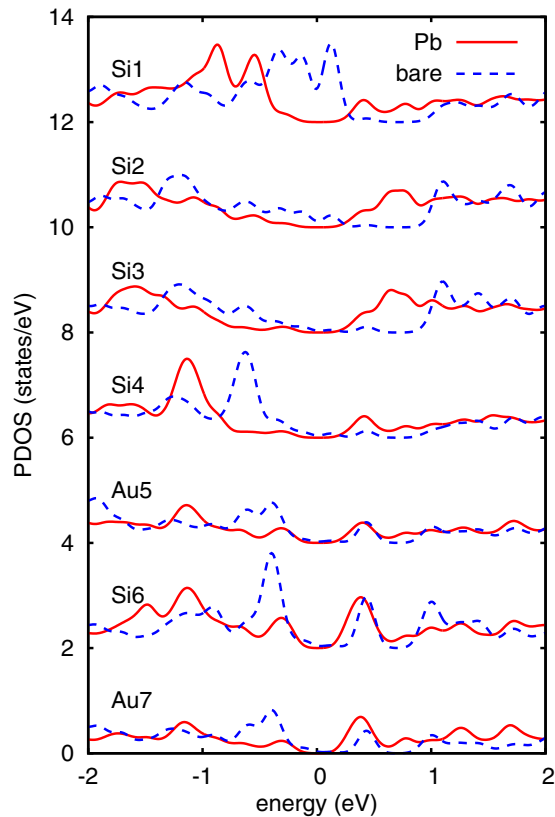
FIG. 9. (Color online) A comparison of calculated PDOS of different surface atoms before and after the adsorption of Pb atom in its lowest energy configuration. For labeling see Fig. 2. All the sets of the curves but Au7 were shifted vertically for clarity. Note a high density of empty states due to the hybridization with Pb atoms.

step-edge Si atom, while protrusion defect was modeled by hydrogen atom bound to one of the step-edge Si atoms. To determine the diffusion barriers we placed a single Pb atom at a given position along the step, fixed its x coordinate (parallel to the steps), and allowed to relax the other two coordinates. Comparing total energies of the system calculated at different positions of Pb atom in the direction parallel to the steps, the diffusion barriers have been determined [28]. Note that such an approach provides only approximate values of the diffusion barriers due to the considered discrete nature of Pb atom positions in the x direction (along step edges). In the present case we took positions with steps of 0.45 Å. The results of calculations are shown in Fig. 10. As it is evident both types of defects can shorten the diffusion channels. In particular, the protrusion at step edge features a high energy barrier ($\sim$0.9 eV) which is twice as high as barriers within the diffusion channel. Thus the defects of this type should repel Pb atoms. So the diffusion channel is determined by the distance between such defects. Most probably such a scenario is realized in
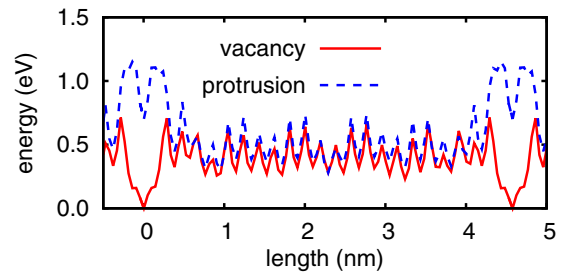

FIG. 10. (Color online) The calculated diffusion barriers along the step edge of the Si(553)-Au surface in the presence of defects: vacancies (red solid curve) and protrusions (blue dashed curve).

experiment. The situation is different in the case of vacancy defects. If Pb atom moves toward the vacancy it may overcome the energy barrier, which is comparable to barriers within the channel, and eventually be trapped in the vacancy. The barrier for the reverse process is in the order of 0.7 eV, thus the vacancy acts as a potential well for Pb atoms, and likely can suppress the diffusion at all. The defects of this type are also observed in experiment. For example see the bright round features in Fig. 1(b), which probably result from trapping Pb atoms into vacancies. All this shows that not only the presence of defects but also the type of defects plays a crucial role in diffusion processes of Pb atoms.

IV. CONCLUSIONS

In conclusion, using the scanning tunneling microscopy and spectroscopy supplemented by density functional theory calculations, we have studied the one-dimensional diffusion of individual Pb atoms along the step edges of the Si(553)-Au surface. The STM and STS measurements show that the movement of Pb atoms is best visible at positive sample bias, which results from a specific electronic structure of Pb adatoms. The present study unambiguously prove that the diffusion channels are limited to a narrow region between Au chains and step edges of the surface. Much wider channels observed in STM and STS data have electronic origin due to the interaction of Pb adatoms with the surface atoms. The length of the channels is determined by a distance between defects at step edges. The defects modify substantially diffusion processes and act as potential barriers or potential wells for Pb atoms, depending on their type.

[1] E. G. Seebauer and C. E. Allen, Prog. Surf. Sci. **49**, 265 (1995).

[2] H. Brune, Surf. Sci. Rep. **31**, 125 (1998).

[3] J. V. Barth, Surf. Sci. Rep. **40**, 75 (2000).

[4] T. T. Tsong, Prog. Surf. Sci. **67**, 235 (2001).

[5] T. Ala-Nissila, R. Ferrando, and S. C. Ying, Adv. Phys. **51**, 949 (2002).

[6] G. Antczak and G. Ehrlich, Surf. Sci. Rep. **62**, 39 (2007).

[7] T. Sato, S. Kitamura, and M. Iwatsuki, Surf. Sci. **445**, 130 (2000).

[8] T. Sato, S. Kitamura, and M. Iwatsuki, J. Vac. Sci. Technol. A **18**, 960 (2000).

[9] H. Uchida, S. Watanabe, H. Kuramochi, J. Kim, K. Nishimura, M. Inoue, and M. Aono, Phys. Rev. B **66**, 161316(R) (2002).

[10] H. Uchida, S. Watanabe, H. Kuramochi, M. Kishida, J. Kim, K. Nishimura, M. Inoue, and M. Aono, Surf. Sci. **532–535**, 737 (2003).

[11] C. M. Chang and C. M. Wei, Phys. Rev. B **67**, 033309 (2003).

[12] J. M. Gómez-Rodriguez, J. J. Sáenz, A. M. Baró, J.-Y. Veuillen, and R. C. Cinti, Phys. Rev. Lett. **76**, 799 (1996).

[13] O. Custance, S. Brochard, I. Brihuega, E. Artacho, J. M. Soler, A. M. Baró, and J. M. Gómez-Rodriguez, Phys. Rev. B **67**, 235410 (2003).

[14] J. Slezák, M. Ondřejček, Z. Chvoj, V. Cháb, H. Conrad, S. Heun, Th. Schmidt, B. Ressel, K. C. Prince, Phys. Rev. B **61**, 16121 (2000).

[15] J. Mysliveček, P. Sobotik, I. Oštádal, T. Jarolimek, and P. Šmilauer, Phys. Rev. B **63**, 045403 (2001).

[16] K. Wang, G. Chen, C. Zhang, M. M. T. Loy, and X. Xiao, Phys. Rev. Lett. **101**, 266107 (2008).

[17] R.-L. Lo, I.-S. Hwang, M.-S. Ho, and T. T. Tsong, Phys. Rev. Lett. **80**, 5584 (1998).

[18] R.-L. Lo, M.-S. Ho, I.-S. Hwang, and T. T. Tsong, Phys. Rev. B **58**, 9867 (1998).

[19] C. Polop, E. Vasco, J. A. Martin-Gago, and J. L. Sacedón, Phys. Rev. B **66**, 085324 (2002).

[20] R. Zhachuk, S. Teys, B. Olshanetsky, and S. Pereira, Appl. Phys. Lett. **95**, 061901 (2009).

[21] R. Zhachuk, B. Olshanetsky, J. Coutinho, and S. Pereira, Phys. Rev. B **81**, 165424 (2010).

[22] I. Brihuega, M. M. Ugeda, and J. M. Gómez-Rodriguez, Phys. Rev. B **76**, 035422 (2007).

[23] T. Hasegawa and S. Hosoki, Phys. Rev. B **54**, 10300 (1996).

[24] E. Bussmann, S. Bockenhauer, F. J. Himpsel, and B. S. Swartzentruber, Phys. Rev. Lett. **101**, 266101 (2008).

[25] P. G. Kang, H. Jeong, and H. W. Yeom, Phys. Rev. B **79**, 113403 (2009).

[26] P. Nita, M. Jałochowski, M. Krawiec, and A. Stępniak, Phys. Rev. Lett. **107**, 026101 (2011).

[27] M. Krawiec and M. Jałochowski, Phys. Rev. B **87**, 075445 (2013).

[28] A. Podsiadły-Paszkowska and M. Krawiec, Surf. Sci. **622**, 9 (2014).

[29] J. N. Crain, J. L. McChesney, F. Zheng, M. C. Gallagher, P. C. Snijders, M. Bissen, C. Gundelach, S. C. Erwin, and F. J. Himpsel, Phys. Rev. B **69**, 125401 (2004).

[30] M. Krawiec, Phys. Rev. B **81**, 115436 (2010).

[31] S. C. Erwin and F. J. Himpsel, Nat. Commun. **1**, 58 (2010).

[32] P. Nita, G. Zawadzki, M. Krawiec, and M. Jałochowski, Phys. Rev. B **84**, 085453 (2011).

[33] J. P. Perdew and A. Zunger, Phys. Rev. B **23**, 5048 (1981).

[34] P. Ordejon, E. Artacho, and J. M. Soler, Phys. Rev. B **53**, R10441 (1996).

[35] D. Sanchez-Portal, P. Ordejon, E. Artacho, and J. M. Soler, Int. J. Quantum Chem. **65**, 453 (1997).

[36] E. Artacho, D. Sanchez-Portal, P. Ordejon, A. Garcia, and J. M. Soler, Phys. Status Solidi B **215**, 809 (1999).

[37] J. M. Soler, E. Artacho, J. D. Gale, A. Garcia, J. Junquera, P. Ordejon, and D. Sanchez-Portal, J. Phys. Condens. Matter **14**, 2745 (2002).

[38] E. Artacho, E. Anglada, O. Dieguez, J. D. Gale, A. Garcia, J. Junquera, R. M. Martin, P. Ordejon, J. M. Pruneda, D. Sanchez-Portal, and J. M. Soler, J. Phys. Condens. Matter **20**, 064208 (2008).

[39] N. Troullier and J. L. Martins, Phys. Rev. B **43**, 1993 (1991).

[40] K. Palotás, G. Mándi, and L. Szunyogh, Phys. Rev. B **86**, 235415 (2012).

[41] G. Mándi, N. Nagy, and K. Palotás, J. Phys. Condens. Matter **25**, 445009 (2013).

[42] K. Palotás, G. Mándi, and W. A. Hofer, Front. Phys. (2013), doi:10.1007/s11467-013-0354-4.

[43] G. Teobaldi, E. Inami, J. Kanasaki, K. Tanimura, and A. L. Shluger, Phys. Rev. B **85**, 085433 (2012).